ORIGINAL ARTICLE

Journal of Cachexia, Sarcopenia and Muscle 2021; **12**: 192–208
Published online 25 November 2020 in Wiley Online Library (wileyonlinelibrary.com) **DOI:** 10.1002/jcsm.12650

TAK1 inhibition improves myoblast differentiation and alleviates fibrosis in a mouse model of Duchenne muscular dystrophy

Dengqiu Xu[1], Sijia Li[1], Lu Wang[1], Jingwei Jiang[1], Lei Zhao[3], Xiaofei Huang[1], Zeren Sun[1], Chunjie Li[1], Lixin Sun[1], Xihua Li[3]*, Zhenzhou Jiang[1,4]* & Luyong Zhang[1,2,4]*

[1]*Jiangsu Key Laboratory of Drug Screening, China Pharmaceutical University, Nanjing, China,* [2]*Center for Drug Research and Development, Guangdong Pharmaceutical University, Guangzhou, China,* [3]*Department of Neurology, Children's Hospital of Fudan University, Shanghai, China,* [4]*Key Laboratory of Drug Quality Control and Pharmacovigilance, China Pharmaceutical University, Nanjing, China*

Abstract

Background Transforming growth factor-β-activated kinase 1 (TAK1) plays a key role in regulating fibroblast and myoblast proliferation and differentiation. However, the TAK1 changes associated with Duchenne muscular dystrophy (DMD) are poorly understood, and it remains unclear how TAK1 regulation could be exploited to aid the treatment of this disease.

Methods Muscle biopsies were obtained from control donors or DMD patients for diagnosis (n = 6 per group, male, 2–3 years, respectively). Protein expression of phosphorylated TAK1 was measured by western blot and immunofluorescence analysis. In vivo overexpression of TAK1 was performed in skeletal muscle to assess whether TAK1 is sufficient to induce or aggravate atrophy and fibrosis. To explore whether TAK1 inhibition protects against muscle damage, mdx (loss of dystrophin) mice were treated with adeno-associated virus (AAV)-short hairpin TAK1 (shTAK1) or NG25 (a TAK1 inhibitor). Serum analysis, skeletal muscle performance and histology, muscle contractile function, and gene and protein expression were performed.

Results We found that TAK1 was activated in the dystrophic muscles of DMD patients (n = 6, +72.2%, $P < 0.001$), resulting in fibrosis (+65.9% for fibronectin expression, $P < 0.001$) and loss of muscle fibres (−32.5%, $P < 0.01$). Moreover, TAK1 was activated by interleukin-1β, tumour necrosis factor-α, and transforming growth factor-β1 ($P < 0.01$). Overexpression of TAK1 by AAV vectors further aggravated fibrosis (n = 8, +39.6% for hydroxyproline content, $P < 0.01$) and exacerbated muscle wasting (−31.6%, $P < 0.01$) in mdx mice; however, these effects were reversed in mdx mice by treatment with AAV-short hairpin TAK1 (shTAK1) or NG25 (a TAK1 inhibitor). The molecular mechanism underlying these effects may be related to the prevention of TAK1-mediated transdifferentiation of myoblasts into fibroblasts, thereby reducing fibrosis and increasing myoblast differentiation.

Conclusions Our findings show that TAK1 activation exacerbated fibrosis and muscle degeneration and that TAK1 inhibition can improve whole-body muscle quality and the function of dystrophic skeletal muscle. Thus, TAK1 inhibition may constitute a novel therapy for DMD.

Keywords TAK1; Duchenne muscular dystrophy; Fibrosis; Differentiation

Received: 26 April 2020; Revised: 9 October 2020; Accepted: 2 November 2020
**Correspondence to: Luyong Zhang and Zhenzhou Jiang, Key Laboratory of Drug Quality Control and Pharmacovigilance, China Pharmaceutical University, Nanjing 210009, China. Email: lyzhang@cpu.edu.cn; beaglejiang@cpu.edu.cn*
Xihua Li, Department of Neurology, Children's Hospital of Fudan University, Shanghai 200032, China. Email: xihual@vip.sina.com

Introduction

Duchenne muscular dystrophy (DMD) is the most common type of fatal muscular dystrophy, with a worldwide incidence of 1 per 5000 live male births.[1] DMD is caused by loss-of-function mutations in the dystrophin gene; these cause defects in the dystrophin protein, which results in progressive muscle degeneration. Typically, DMD develops within the first 3–5 years of life, where progressive muscle weakness impairs walking ability; patients typically die because of respiratory failure or cardiac failure.[2,3] Some studies have shown that the progressive muscle deterioration characterizing DMD is caused by progressive loss of muscular fibres and concomitantly increased inflammation and fibrosis.[4,5] No pharmacological treatment for DMD is available, although gene therapy to repair or replace the defective dystrophin gene represents a promising approach. The full-length dystrophin gene poses the greatest challenge because it exceeds the packaging limit of viral vectors.[6] Thus, there is a need for discovery of small molecule drugs that may effectively treat DMD.

Fibrosis in skeletal muscle is one of the typical injuries associated with DMD, a condition characterized by muscle degeneration and subsequent loss of mobility.[7,8] Fibroblasts are continuously activated in DMD, resulting in massive collagen deposition.[9] As a key mediator of fibrosis, fibroblasts are activated by transforming growth factor (TGF)-β1 during chronic injury.[10] Many studies have shown that TGF-β1 increases significantly in the muscles of DMD patients, and TGF-β1 inhibition has been suggested as a potential approach to alleviate fibrosis in DMD.[11,12] However, no effective clinical drugs targeting TGF-β1 are available to attenuate fibrosis in DMD patients. Other inflammatory cytokines also induce inflammatory responses that contribute to fibrosis[13]; thus, drugs that target TGF-β1 alone may not completely halt fibrosis. Thus, there is an urgent need to develop a drug that prevents inflammatory cytokine-mediated profibrotic activities.

Children with DMD ultimately die because of muscle wasting, where muscle is replaced by collagen and fat tissue. Alleviating muscle fibrosis and promoting myoblast differentiation into myofibres could serve as novel treatment strategies for DMD. We aimed to identify a therapeutic target not only to control fibrosis but also to regulate myoblast differentiation. TGF-β-activated kinase 1 (TAK1), a member of the mitogen-activated protein kinase (MAPK) kinase family, was found to play a role in MAPK activation.[14] Studies have shown that TAK1 is activated by TGF-β1, interleukin (IL)-1β, and tumour necrosis factor-α (TNF-α), thus promoting fibrosis via the p38-MAPK signalling pathway.[15,16] Moreover, a recent study provided evidence of impaired myoblast growth in association with excessive production of TGF-β1 in DMD, but it remains unknown whether this was related to TAK1.[11] These reports led us to hypothesize that TAK1 may contribute to the accumulation of fibrosis and inhibition of myoblast differentiation. We explored this possibility by assaying the TAK1 level in the skeletal muscle of DMD patients and mdx mice. Our findings suggest that TAK1 regulation may be exploited to aid treatment of DMD.

Materials and methods

Patients and study design

Triceps muscle biopsies were obtained from control donors who underwent orthopaedic surgery (n = 6) and DMD patients (n = 6) matched for age (2–3 years). For DMD patients, triceps muscle biopsies were obtained for diagnosis. All of the biopsies were obtained from the Children's Hospital of Fudan University (Shanghai, China), and all participants provided written informed consent prior to initiation of study procedures. The serum samples from healthy donors (n = 13) and DMD patients (n = 13) without obtained drug treatment (2–8 years). This study is a registered clinical trial at Children's Hospital of Fudan University (NCT number: 2019-244).

Animal studies

Dystrophin-deficient C57BL/10ScSnJNju-Dmdem3Cd4/Gpt (mdx) mice and C57BL/10ScSn/J strain controls were purchased from the Animal Model Research Center of Nanjing University (Nanjing, China). All comparisons were made between age-matched male mice. Experiment 1 included 16 male mdx mice aged 3–4 weeks that were randomly allocated to adeno-associated virus (AAV)-control mdx and AAV-TAK1 mdx groups; their normoglycaemic littermates (n = 16; all males aged 3–4 weeks) were randomly allocated to AAV-control control and AAV-TAK1 control groups. Experiment 2 included 18 male mdx mice aged 3–4 weeks that were randomly allocated to AAV-short hairpin RNA (shRNA)-control and AAV-shRNA-TAK1 groups; their normoglycaemic littermates (n = 9; all males aged 3–4 weeks) served as the control group. A schematic diagram of the animal experimental design is shown in *Figure* 6A. Experiment 3 included 18 male mdx mice aged 3–4 weeks and their normoglycaemic littermates (n = 9; all males aged 3–4 weeks), and the aim was to determine the effects of NG25 on DMD. The 18 mdx mice were randomly divided into two groups of nine mice each: a control group and an NG25 group (6 mg/kg/day intraperitoneally for 2 weeks), as shown in *Figure* 8A. After 2 weeks, the mice were euthanized. The tibialis anterior (TA) and diaphragm (DIA) muscle sections were subjected to histological and western blot analysis.

Recombinant adeno-associated virus

Adeno-associated virus-muscle creatine kinase (CK)-TAK1-eGFP (AAV2/9, 1.0×10^{13} genomic copies per millilitre) were made by Hanbio, which were used to overexpress TAK1 in mice. A single dose of AAV-TAK1 vector (5×10^{11} vg particles/100 μL/mouse) was delivered to control and mdx mice via tail vein injection. Production and purification of recombinant AAV were made by Hanbio. Mice were evaluated after treatment for 4 weeks.

A single dose of 1.1×10^{12} vg/mice in 100 μL of AAV2/9 expressing shTAK1 was delivered to mdx mice via tail vein injection, and the same dose of AAV2/9 expressing shRNA control was injected as AAV-shRNA control group. The shRNA oligonucleotides were synthesized to contain the sense strand of target sequences for mouse TAK1 (5′-GGTGCTGAACCATTGCCTTAC-3′) and mouse shRNA control (5′-GGGCTATCCCAACGCTATTAGT-3′). Production and purification of recombinant AAV were made by Hanbio (Shanghai, China). Four weeks later, mice were euthanized and visualized by confocal imaging.

In vivo muscle strength test and wire grip test

Step length was measured by painting the forelimb/hind feet of mice as reported previously.[17] In brief, mice run a small corridor lined with paper approximately 1.2 m in length. Distance between steps of the same foot were measured and averaged over five consecutive runs, excluding areas of stoppage. Forelimb grip strength test was used to assay the grip strength of forelimb using a calibrated grip strength tester (YLS-13A, Yiyan Bio, Shandong, China). All tests were performed as described previously.[18] The grip strength analysis was reported as the mean of at least three repetitions. A wire test is a typical method to assess muscle condition and the whole-body force in mice. The wire grip test was performed at 2 days before mice were sacrificed. All mice were allowed to grasp a 2 mm diameter metal wire, and the length of time was recorded until the mice fell. The test score was calculated as the mean of at least three repetitions.

Skeletal muscle contractile function

Tibialis anterior strength (specific force) and fatigue resistance were measured by using a length control system (BL-420, Techman Scientific). After determining the optimum length by tetanic contractions as descried previously,[19] the TA muscles then underwent a fatigue protocol, in which the TA muscles were subjected to repeated stimulation at 120 Hz (200 ms duration) every 2 s for a total of 2 min. One minute late fatigue recovery was assessed every 2 min up to total 10 min after fatigue.[20]

Blood biochemical analysis

Blood was collected from the inferior vena cava before the mice were euthanized. Blood samples were centrifuged at 1500 g for 10 min at 4°C and then used to measure serum CK activity level and plasma lactic dehydrogenase (LDH) level by using an HITACHI7080 Automatic Clinical Analyser (Tokyo, Japan).

Enzyme-linked immunosorbent assay

Serum IL-1β, TNF-α, and TGF-β1 contents were detected by enzyme-linked immunosorbent assay (ELISA) analysis. Before the assay, the latent form of TGF-β1 contained in human or mouse serum was activated to the immunoreactive form using 1N HCl for acid activation and 1.2N NAOH/0.5 M HEPES for neutralization. The sandwich ELISA of IL-1β, TNF-α, and TGF-β1 were performed according to the manufacturer's instructions. The human ELISA kits were purchased from Fcmacs Biotech Co., Ltd. (Nanjing, China). The mouse ELISA kits were purchased from BioSource (Nivelles, Belgium).

Real-time quantitative PCR

Total RNA was isolated from the fresh TA muscle using TRIzol reagent and an RNeasy Kit (Vazyme Biotech, Nanjing, China). Complementary DNA was synthesized from total RNA using complementary DNA synthesis kit (Vazyme Biotech, Nanjing, China) following the manufacturer's instructions. Real-time PCR was performed using SYBR Green as previously reported.[21] Gene expression was calculated by the ΔΔCT method using glyceraldehyde 3-phosphate dehydrogenase as the reference gene. All primer pairs used for the PCR are listed in Supporting Information, *Table* S1.

Histological analysis

Cryosections of TA muscle were mounted on a slide and then transversely sectioned into 5 μm slices. After staining with haematoxylin and eosin (HE) following standard protocols, the slides were viewed and photomicrographs were captured under light microscope (BX53, Olympus, Japan).

Hydroxyproline fibrosis assay

To quantify muscle fibrosis, collagen I content was measured by using the hydroxyproline assay as described previously.[22] Hydroxyproline values were normalized to the total protein content of the muscle.

Western blot analysis

Western blot analysis was performed as described previously.[20] In brief, protein extracts were fractionated on 6–12% sodium dodecyl sulphate polyacrylamide gels and transferred onto polyvinylidene fluoride membranes (Millipore, Billerica, MA, USA) via electroblotting. The membranes were blocked in Tris-buffered saline containing 5% bovine serum albumin for 90 min at room temperature. Next, membranes were incubated with the primary antibody at 4°C overnight. Signals were detected using a BioRad Chemiluminescent Imaging System (Hercules, CA, USA). The information of all antibodies was listed in Supporting Information, *Table* S2.

Isolated myoblasts

Human primary myoblasts were obtained from the triceps muscles of DMD patients, and mouse myoblasts were extracted from the extensor extensor digitorum longus (EDL) or DIA muscles. Myoblasts were isolated using 1.2 U/mL dispase (D4693; Sigma-Aldrich, St. Louis, MO, USA) and 5 mg/mL collagenase type D (35799223; Roche Diagnostics Ltd., Shanghai, China), and the cells were filtered using a 40 μm strainer. Then, Pax7-stained cells were collected through a Miltenyi LS magnetic column (130-042-401; Miltenyi, Shanghai, China). Isolated myoblasts were cultured in Dulbecco's modified Eagle's medium containing 20% foetal bovine serum, 1% chicken embryo extract, and 10% horse serum (Gibco), as described previously.[18]

Immunofluorescence

Fresh TA muscle cryosections were mounted on a slide and blocked in blocking buffer for 60 min. Samples (myoblasts, myofibres, and cryosections) were fixed in paraformaldehyde (PFA) 4% for 1 h. Then, samples were incubated overnight with primary antibody against fibronectin (1:200; ab32419, Abcam), myosin heavy chain (MHC) (1:200; MF 20, Developmental Studies Hybridoma Bank, Iowa City, IA, USA), Pax7 (1:100; sc-52903, Santa Cruz), and myogenin (1:100; sc-81648, Santa Cruz) at 4°C. Next, these samples were incubated with secondary antibody (Alexa Fluor 633, Alexa Fluor 488; Thermo, Waltham, MA, USA). 4′,6-Diamidino-2-phenylindole (DAPI) was used to visualize nuclei. The sections were viewed, and photomicrographs were captured under fluorescence microscope (FV1000, Olympus, Japan).

Statistical analysis

Unpaired Student's *t*-test was used to compare values between two groups. Other data were analysed by one-way or two-way analysis of variance followed by Tukey's multiple comparison test, performed using GraphPad software (ver. 8.0; GraphPad Software Inc., La Jolla, CA, USA). Data are presented as the mean ± SEM. P values < 0.05 were considered statistically significant.

Results

Fibrosis and atrophy of the muscles of Duchenne muscular dystrophy patients are accompanied by TAK1 activation

First, the dystrophic status of the muscles of DMD patients was confirmed via dystrophin immunofluorescence staining of the triceps muscle (Supporting Information, *Figure* S1A). The degree of muscle damage was indexed by the plasma CK level, which showed a significant increase in DMD patients (*Figure* S1B). It is well known that fibrosis is a major cause of muscle weakness in DMD patients.[23] HE staining of the triceps muscle revealed significant fibrosis and inflammation (*Figure* S1C). The fibrosis was confirmed via fibronectin immunofluorescence analysis and calculation of the fibrosis index (*Figure* 1A and 1B). We measured the fibronectin protein level via western blotting; the level was significantly elevated in the triceps muscle of DMD patients compared with controls (*Figure* 1C and 1D). Moreover, immunofluorescence analysis revealed a significant reduction in the expression of MHC (a known myogenic marker) and an increase in the expression of embryonic MHC (eMyHC), in the triceps muscles of the DMD patients (*Figure* 1E and 1F), as confirmed by western blotting (*Figure* 1G and 1H). Muscle wasting and atrophy were attributable to increased expression of muscle RING-finger 1 (MuRF1),[24] the level of which was significantly higher (compared with controls) in the triceps muscle of DMD patients (*Figure* S1D and S1E). The TAK1 signalling pathway plays a vital role in inflammation and fibrosis.[25,26] Western blot and immunofluorescence analysis revealed that TAK1 was expressed in the triceps muscle of DMD patients. The levels of phosphorylated TAK1 (p-TAK1) and total TAK1 (t-TAK1) were increased in the triceps muscle of DMD patients compared with controls (*Figure* 1I–1K). TAK1 was activated by TGF-β1, and the muscles of DMD patients showed higher TGF-β1 expression than those of controls, based on western blotting and immunofluorescence analysis (*Figure* S1F and S1G). Together, the results indicate that fibrosis in and atrophy of the muscles of DMD patients are accompanied by TAK1 activation.

Muscle fibrosis and atrophy in mdx mice are accompanied by TAK1 activation

In mdx mice, the soleus (SOL) muscle contains more oxidative type I fibres; the TA muscle can be considered as

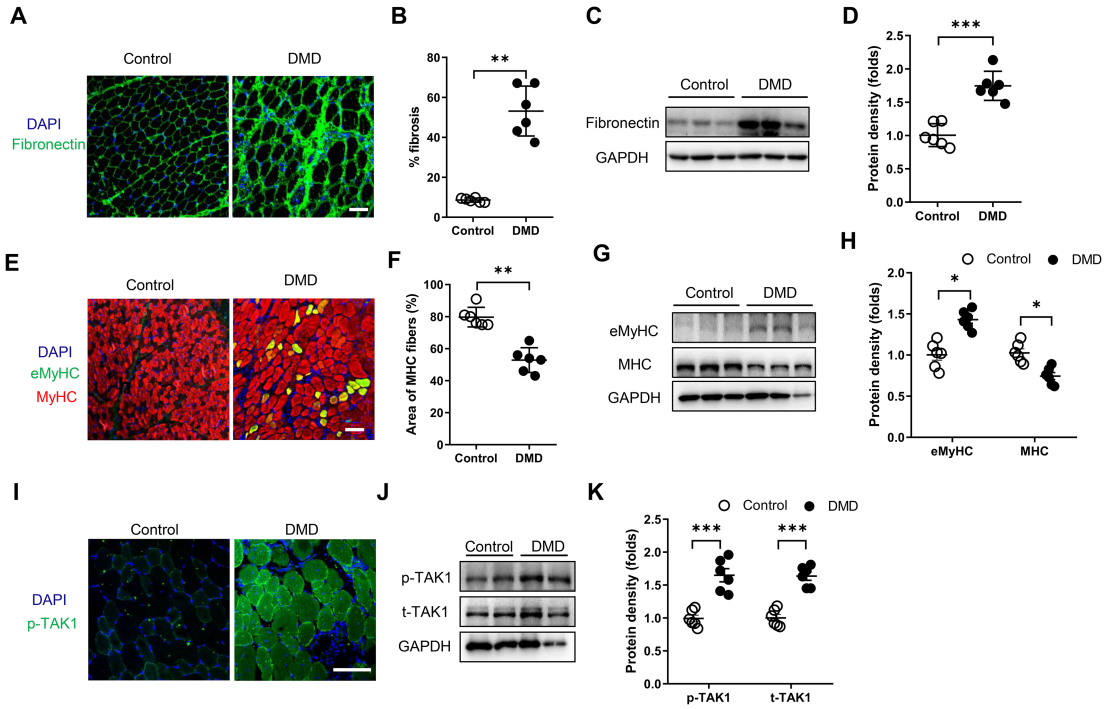

Figure 1 Fibrosis in and atrophy of the muscles of DMD patients is accompanied by TAK1 activation. (A) Fluorescent fibronectin-stained triceps of controls and DMD patients, and nuclei are stained with DAPI (blue). The fibrosis index was calculated as percent of fibrosis = fibronectin area/total area. Scale bar, 100 μm. (B) Percentage of fibrosis in healthy and DMD muscles as measured by fibronectin immunostaining in muscle sections. (C and D) Western blot of fibronectin protein level and the pooled values. (E) Representative images of MHC (red), embryonic myosin heavy chain (eMyHC) immunostaining, and nuclei are stained with DAPI (blue). Scale bar, 100 μm. (F) The percentages of MHC positive areas (red) calculated using InnerView 2.0 software. (G and H) Western blot of eMyHC and MHC protein levels in triceps of controls and DMD patients. (I) Fluorescent p-TAK1 (green)-stained triceps sections of controls and DMD patients, and nuclei are stained with DAPI (blue). Scale bar, 100 μm. (J and K) Western blot of p-TAK1 (Thr-184/187) and t-TAK1 protein levels in triceps of controls and DMD patients. Values are expressed as means ± standard deviation (SD) ($n = 6$), *$P < 0.05$ vs. controls. DAPI, 4′,6-diamidino-2-phenylindole; DMD, Duchenne muscular dystrophy; eMyHC, embryonic myosin heavy chain; GAPDH, glyceraldehyde 3-phosphate dehydrogenase; MyHC, myosin heavy chain; TAK1, transforming growth factor-β-activated kinase 1.

representative of the whole-body muscle quality (in terms of the muscle fibre composition), and DIA muscle is the most affected muscle in mdx mice.[27] Thus, the present investigation of the relationship between TAK1 activity and muscle damage was based on the SOL, TA, and DIA muscles. The TAK1 level followed the order DIA > TA > SOL, whereas the MHC level was in the order SOL > TA > DIA in the mdx mice (*Figure* 2A and 2B). As expected, the extent of inflammation and fibrosis in the mdx mice were also in the order DIA > TA > SOL, as shown by HE, Masson's, and fibronectin immunofluorescence staining (*Figure* 2C–2E). Taken together, these results show that muscle damage in mdx mice is accompanied by TAK1 activation.

TAK1 is activated by IL-1β, TNF-α, and TGF-β1

Studies have shown that TGF-β1-mediated fibronectin and collagen expression in kidney, heart, and dermal mesenchymal cells involves TAK1 activation.[28,29] In this study, TAK1 was activated in the muscles of DMD patients and mdx mice, presumably via IL-1β, TNF-α, and TGF-β1. To test this, we measured the serum levels of these cytokines using ELISA kits. The serum levels of IL-1β, TNF-α, and TGF-β1 were all increased in DMD patients (*Figure* 3A–3C) and mdx mice (Supporting Information, *Figure* S2A–S2C). Next, we established primary myoblast cultures from DMD patients and mdx mice. Treatment of the primary myoblasts from DMD patients (*Figure* 3D and 3E) with IL-1β, TNF-α, and TGF-β1 (doses of 1–20 ng/mL) resulted in dose-dependent TAK1 activation and phosphorylation. These results were repeated in the primary myoblasts from mdx mice (*Figure* S2D and S2E). Thus, cytokines (IL-1β, TNF-α, and TGF-β1) secreted as part of the inflammatory response in DMD promote TAK1 activation and phosphorylation.

TAK1 regulates myoblast differentiation and fibrosis in primary myoblasts

To further investigate the relationships of TAK1 activation with myoblast differentiation and fibrosis, we examined myoblast differentiation and fibrosis in primary myoblasts from mdx mice following TAK1 activation by TGF-β1 (doses of

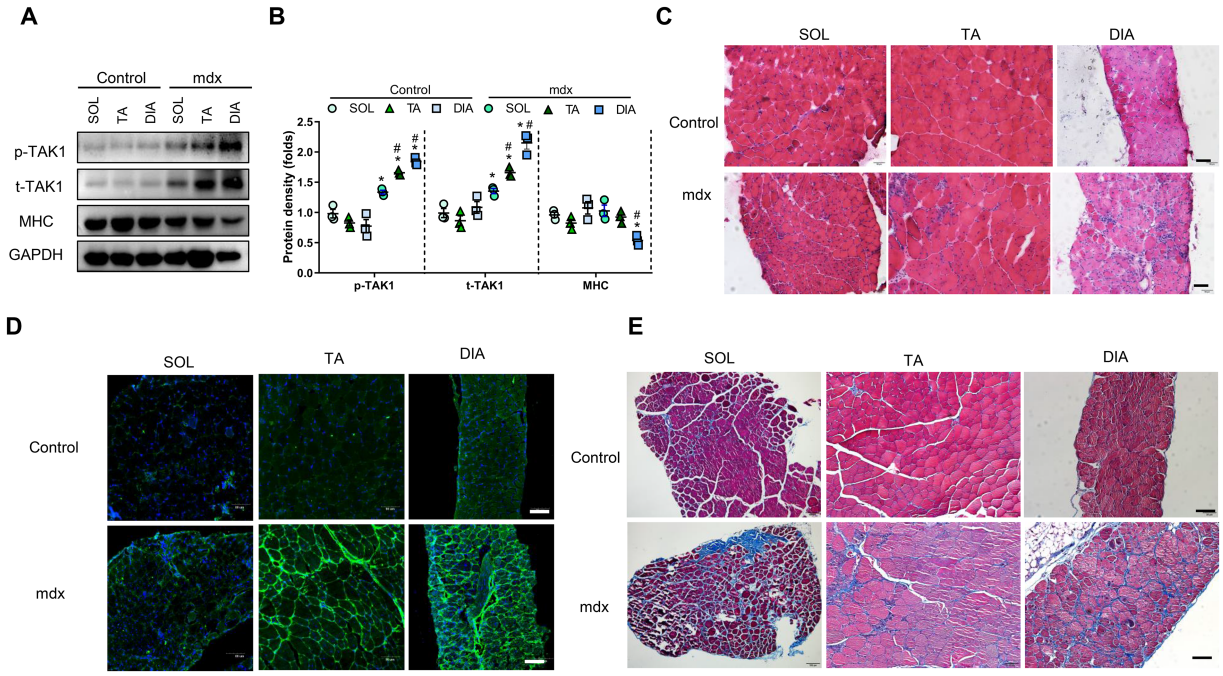

Figure 2 Muscle fibrosis and atrophy in mdx mice are accompanied by TAK1 activation. (A and B) Western blot of p-TAK1, t-TAK1, and myosin heavy chain (MHC) protein levels in SOL, EDL, and DIA muscles of control mice or mdx mice aged 6 weeks (n = 3). (C) Representative HE stained images of SOL, EDL, and DIA muscles for both control mice and mdx mice. Scale bar, 100 μm (n = 6). (D and E) Representative fibronectin's (green) stained images and Masson's stained images of SOL, EDL, and DIA muscles for both control mice and mdx mice, and nuclei are stained with DAPI (blue). Scale bar, 100 μm (n = 6). Values are expressed as means ± standard deviation (SD), $^{*}P < 0.05$, $^{**}P < 0.01$ vs. SOL muscle. DIA, diaphragm; GAPDH, glyceraldehyde 3-phosphate dehydrogenase; MHC, myosin heavy chain; p-TAK1, phosphorylated transforming growth factor-β-activated kinase 1; SOL, soleus; t-TAK1, total transforming growth factor-β-activated kinase 1; TA, tibialis anterior.

1–5 ng/mL). Western blot analysis revealed a reduction in the myogenin level, and a significant increase in the myostatin level, after TAK1 activation in primary myoblasts following treatment with TGF-β1 (Supporting Information, *Figure* S3A and S3B). Moreover, TAK1 activation by TGF-β1 increased MuRF1 expression and decreased MHC expression. Furthermore, TGF-β1-induced TAK1 activation increased collagen I expression (*Figure* S3C and S3D). In summary, TAK1 activation may inhibit myoblast differentiation and increase fibrosis.

It is still unknown whether TAK1 inhibitors can reverse the TGF-β1-induced decrease in differentiation and increase in fibrosis. To test this, primary myoblasts were treated with TGF-β1 in the presence or absence of NG25 (a TAK1 inhibitor). We found that TGF-β1-induced TAK1 phosphorylation was attenuated by treatment with NG25 (doses of 1–10 μM). Moreover, NG25 inhibited the transdifferentiation of myoblasts into fibroblasts, as indicated by reduced collagen I protein expression (*Figure* 4A and 4B). In addition, NG25 promoted myoblast differentiation, as revealed by decreased myostatin expression and increased myogenin expression (*Figure* 4A and 4B). This enhancement of differentiation by NG25 was confirmed by myogenin and MHC immunofluorescence staining (*Figure* 4C and 4D). To further investigate whether TAK1 activation could induce myoblasts transdifferentiation, we performed immunostaining with collagen I and Pax7. We found that the percentage of $Pax7^{+}$ collagen I^{+} cells increased after TGF-β1 treatment (*Figure* 4E and 4F). In addition, primary myoblasts exhibited decreased MHC level but an increased alpha-smooth muscle actin (α-SMA) level after TGF-β1 treatment (*Figure* 4G and 4H). Moreover, these effects were offset by NG25 treatment. We suppose that TAK1 activation could induce transdifferentiation of myoblasts.

TAK1 activation attenuates myoblast differentiation and aggravates fibrosis in mdx mice

To further investigate the relationships of TAK1 activation with myoblast differentiation and fibrosis in vivo, we used AAV-2/9-TAK1 and enhanced green fluorescent protein (eGFP) to induce and assess TAK1 overexpression in the muscles of both control and mdx mice over a 4-week period. Overexpression of TAK1 had no effect on grip strength (*Figure* 5A) or LDH activity (*Figure* 5B) in either the control or mdx mice and increased the CK level only in mdx mice (*Figure* 5C). Overexpression of p-TAK1 and t-TAK1 in proteins was seen in the TA and DIA muscles of both control and mdx mice (Supporting Information, *Figure* S4A–S4F). TAK1 activation caused damage to the TA and DIA muscles of the control mice

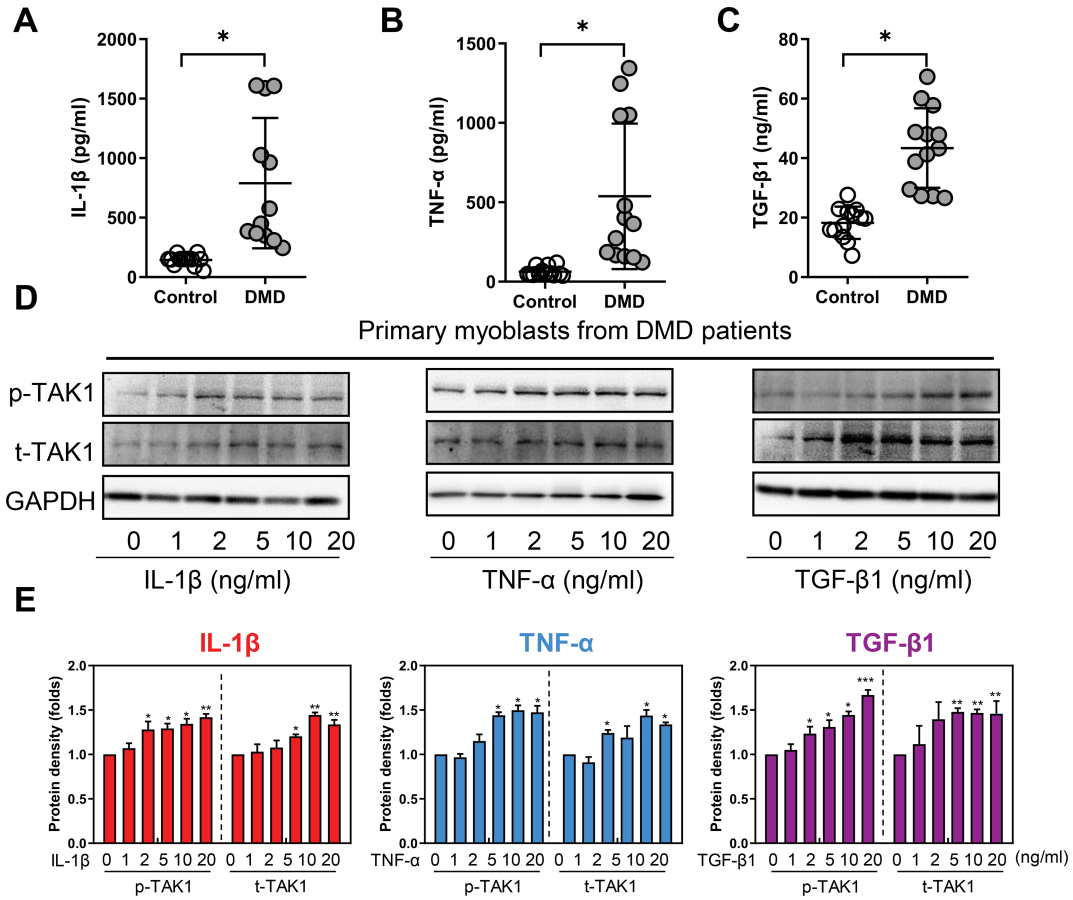

Figure 3 TAK1 is activated in human primary myoblasts by IL-1β, TNF-α, and TGF-β1. (A–C) Serum IL-1β, TNF-α, and TGF-β1 level for control and DMD patients. Values are expressed as means ± standard deviation (SD) (n = 13), $^{*}P < 0.05$, $^{**}P < 0.01$ vs. controls. (D and E) Primary myoblasts isolated from triceps muscle of DMD patients and then myoblasts treated with 0, 1, 2, 5, 10, and 20 ng/mL IL-1β or TNF-α or TGF-β1 for 2 h. Western blot of p-TAK1 and t-TAK1 protein levels and the pooled values for each group. Values are expressed as means ± standard deviation (SD) (n = 3), $^{*}P < 0.05$, $^{**}P < 0.01$, $^{***}P < 0.001$ vs. control group. DIA, diaphragm; DMD, Duchenne muscular dystrophy; GAPDH, glyceraldehyde 3-phosphate dehydrogenase; IL, interleukin; p-TAK1, phosphorylated transforming growth factor-β-activated kinase 1; SOL, soleus; t-TAK1, total transforming growth factor-β-activated kinase 1; TA, tibialis anterior; TNF-α, tumour necrosis factor-α.

according to HE staining (*Figure* S4G) and severely damaged the muscles of mdx mice, as indicated by inflammation and fibrosis in the AAV-TAK1 mdx mouse group. We further evaluated fibrosis by Masson's and fibronectin immunofluorescence staining of the TA and DIA muscles: the AAV-TAK1 control mouse group showed slight fibrosis compared with the AAV-control control mouse group; the AAV-TAK1 mdx mouse group showed more fibrosis than the AAV-control group (*Figure* 5D–5F). These results were confirmed using the hydroxyproline assay (*Figure* 5G). Then, we counted the myofibres via MHC immunofluorescence analysis and observed that TAK1 overexpression decreased the number of myofibres in both control mice and mdx mice (*Figure* 5H and 5I). Together, the data show that TAK1 activation caused fibrosis and muscle wasting in control mice, and TAK1 overexpression further aggravated muscle fibrosis and exacerbated muscle wasting in mdx mice.

TAK1 knockdown improves myoblast differentiation and alleviates fibrosis in mdx mice

Fibrosis and atrophy in DMD patients and mdx mice are associated with TAK1 activation; TAK1 inhibitors could attenuate the TAK1 activation-induced decrease in differentiation and increase in fibrosis in primary myoblasts. We further examined the effects of TAK1 knockdown on myoblast differentiation and fibrosis in mdx mice. AAV-2/9-shRNA-TAK1 was used to knock down TAK1 protein expression in the muscles of mdx mice via intravenous tail injection (Supporting Information, *Figure* S5A). After 4 weeks, eGFP was observed in the TA and DIA muscles of both AAV-shRNA-control mice and AAV-shRNA-TAK1 mice (*Figure* S5B), as confirmed by eGFP fluorescence staining (*Figure* S5C). Next, all mice were subjected to gait analysis (*Figure* 6A) according to a previously published procedure.[17] Stride length was reduced, and the

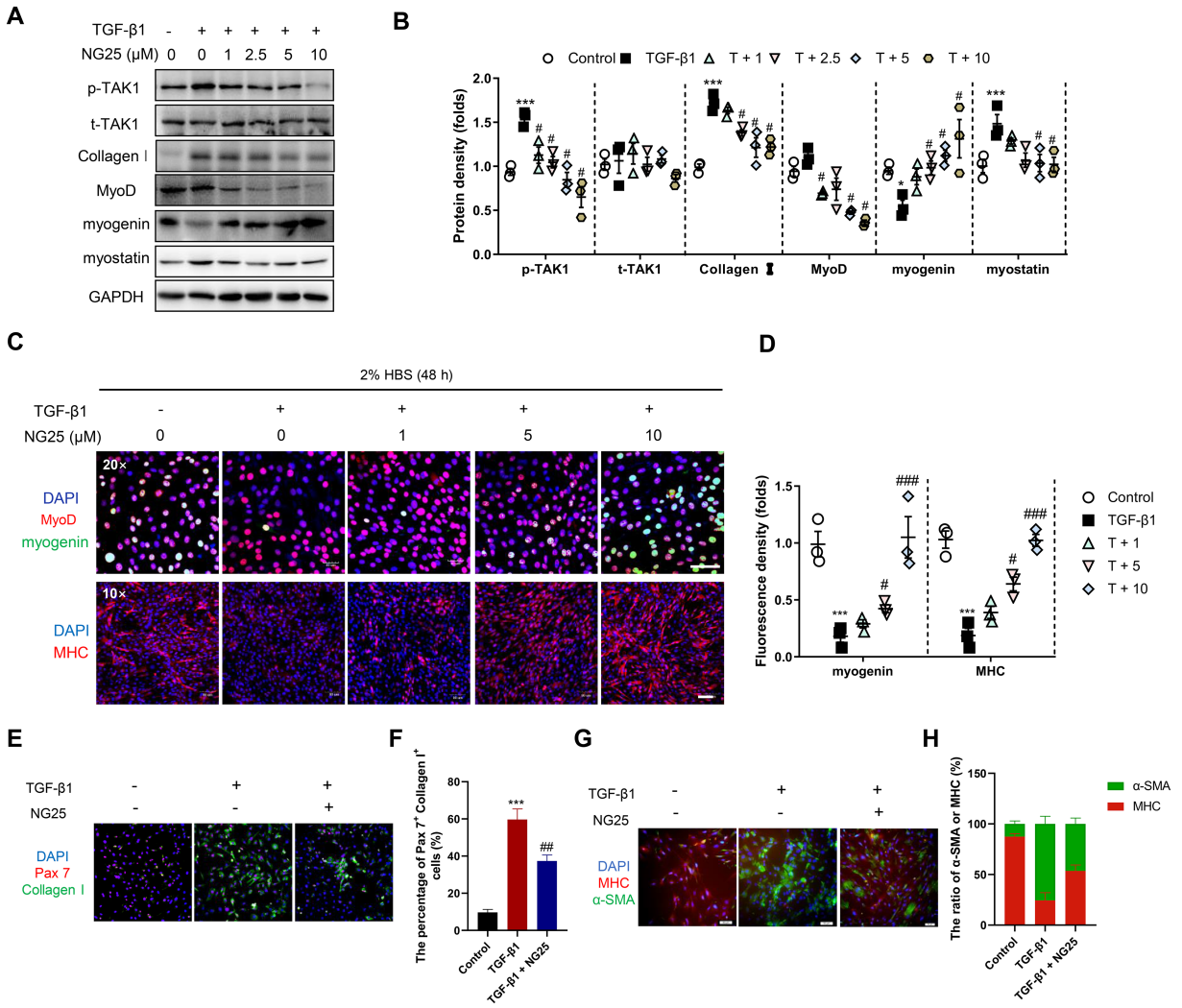

Figure 4 NG25 improved myoblasts differentiation and inhibited fibrosis in primary myoblasts. Primary myoblasts from EDL muscle of mdx mice, then myoblasts treated with TGF-β1 in the presence or absence of NG25 (1, 2.5, 5, and 10 μM). (A and B) Western blot of p-TAK1, t-TAK1, collagen I, MyoD, myogenin, and myostatin protein levels. (C, upper panel) Representative images of MyoD (red), myogenin (green) immunostaining, and nuclei are stained with DAPI (blue). Scale bar, 200 μm. (c, lower panel) Representative images of MHC (red) immunostaining, and nuclei are stained with DAPI (blue). Scale bar, 100 μm. (D) The fluorescence density was calculated using InnerView 2.0 software (T, TGF-β1; T +1, TGF-β1 + 1 μM NG25; T +2.5, TGF-β1 + 2.5 μM NG25; T +5, TGF-β1 + 5 μM NG25). (E) Representative images of Pax7 and collagen I immunostaining and (F) the percentages of Pax7 $^{+}$ collagen I $^{+}$ in each group. (G) Representative images of primary myoblasts expressing MHC and α-SMA with TGF-β1 (10 ng/mL) or NG25 (5 μM) for 48 h in differentiation medium. (H) The ratio of primary myoblasts expressing MHC or α-SMA in each group. Values are expressed as means ± standard deviation (SD) (n = 3), *P < 0.05, **P < 0.01, ***P < 0.001 vs. control group; #P < 0.05, ##P < 0.01, ###P < 0.001 vs. TGF-β1 group. α-SMA, alpha-smooth muscle actin; DAPI, 4′,6-diamidino-2-phenylindole; GAPDH, glyceraldehyde 3-phosphate dehydrogenase; MHC, myosin heavy chain; p-TAK1, phosphorylated transforming growth factor-β-activated kinase 1; t-TAK1, total transforming growth factor-β-activated kinase 1.

stride width of the hindlimbs was increased, in mdx vs. control mice; however, AAV-shRNA-TAK1 reversed these changes (*Figure* 6B and 6C). Furthermore, the muscle function of the AAV-shRNA-control mdx mice showed a decline, which was partially restored by AAV-shRNA-TAK1 treatment, as evidenced in vivo by a 24.9% increase in maximum grip strength and a 33.6% increase in the duration of wire test (*Figure* 6D–6F). Increased muscle fatigue and reduced force are major causes of the muscle weakness that characterizes DMD; we found that AAV-shRNA-TAK1 had no effect on the force of the TA muscle (*Figure* 6G) but aided in its recovery from fatigue (*Figure* 6H and 6I). Moreover, the AAV-shRNA-control mdx mice exhibited TA muscle hypertrophy, which was partially reduced by the AAV-shRNA-TAK1 treatment (*Figure* 6J). In addition, serum CK and LDH levels increased significantly in the AAV-shRNA-control mdx mice, but this was partially attenuated by AAV-shRNA-TAK1 treatment (*Figure* 6K and 6L). Overall, the results show that knockdown of TAK1 can improve muscle quality and performance in mdx mice.

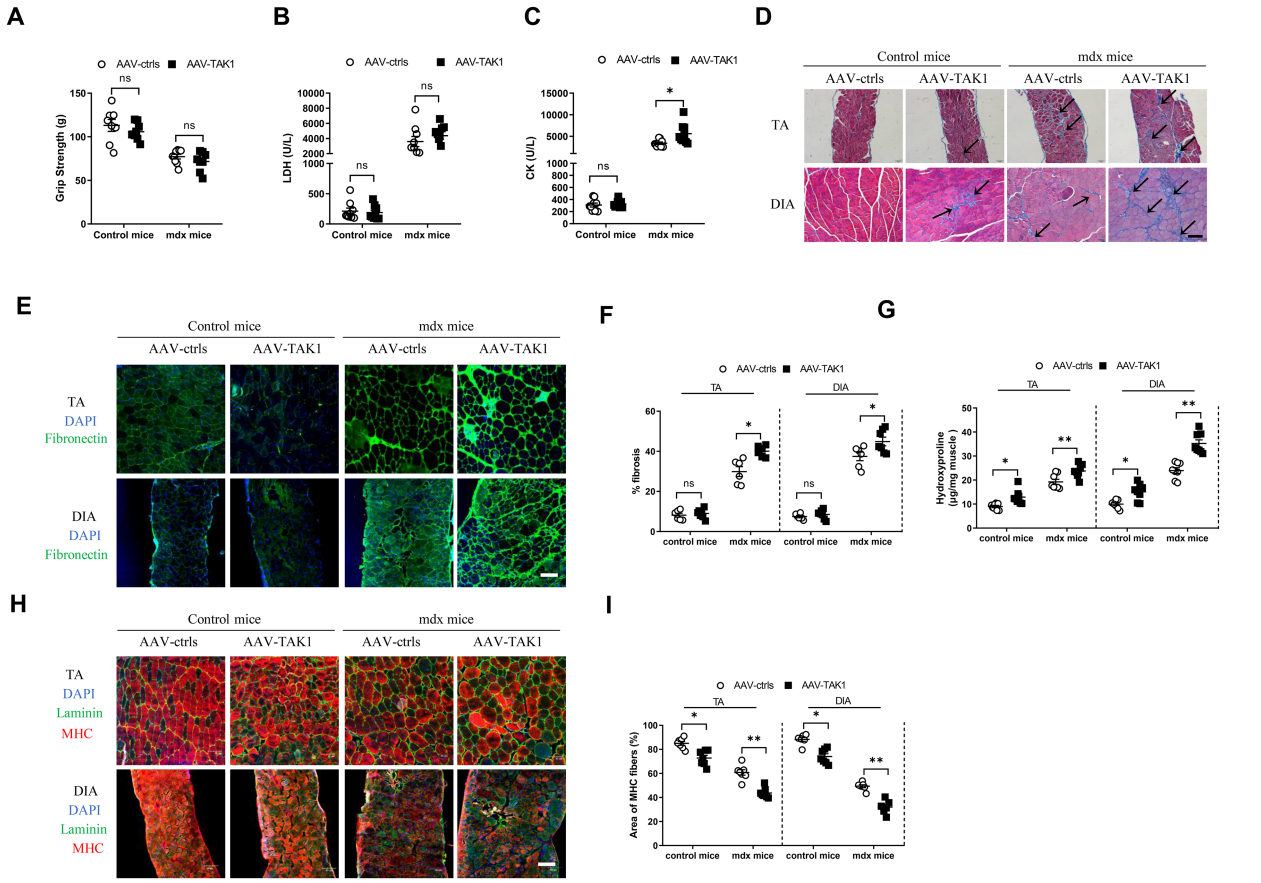

Figure 5 TAK1 activation attenuates myoblast differentiation and exacerbates fibrosis in mdx mice. (A) Grip strength was measured after injection of AAV-TAK1 in control or mdx mice after 4 weeks. (B) Serum LDH and (C) CK activity (n = 8). (D) Representative Masson's trichrome stained imagine of (upper panel) TA and (lower panel) DIA sections. Scale bar, 100 μm (n = 6). (E) Fluorescent fibronectin-stained (upper panel) TA and (lower panel) DIA of mdx mice, and nuclei are stained with DAPI (blue). Scale bar, 100 μm (n = 6). (F) Percentage of fibrosis as measured by fibronectin immunostaining in TA and DIA muscle sections (n = 6). (G) Hydroxyproline content (μg hydroxyproline/mg muscle) in TA and DIA muscles (n = 8). (H) Fluorescent laminin (green) and MHC (red)-stained (upper panel) TA and (lower panel) DIA of mdx mice, and nuclei are stained with DAPI (blue). Scale bar, 100 μm (n = 8). (I) The percentages of MHC positive areas (red) calculated using InnerView 2.0 software (n = 6). Values are expressed as means ± standard deviation (SD), $^{**}P < 0.01$, $^{***}P < 0.001$ vs. control group; $\#P < 0.05$, $\#\#P < 0.01$, $\#\#\#P < 0.001$ vs. AAV-ctrls. AAV, adeno-associated virus; DAPI, 4′,6-diamidino-2-phenylindole; DIA, diaphragm; MHC, myosin heavy chain; SOL, soleus; TAK1, transforming growth factor-β-activated kinase 1; TA, tibialis anterior.

Interleukin-1β, TNF-α, and TGF-β1 levels were all increased in DMD patients (*Figure* 3A–3C) and mdx mice (*Figure* S2A–S2C), which could have been responsible for the TAK1 activation and phosphorylation. To investigate the effects of AAV-shRNA-TAK1 on muscle quality and performance in association with IL-1β, TNF-α, and TGF-β1 expression, we measured the levels of these cytokines using ELISA. AAV-shRNA-TAK1 treatment had no effect on the levels of IL-1β, TNF-α, or TGF-β1 (*Figure* S5D). Therefore, the protective effects of AAV-shRNA-TAK1 in mdx mice were not attributable to reductions in the levels of inflammatory cytokines.

In TA muscle, we found increased levels of p-TAK1 and t-TAK1 in the AAV-shRNA-control mdx; however, these increases were significantly reduced by AAV-shRNA-TAK1 treatment (*Figure* 7A). In DIA muscle, AAV-shRNA-TAK1 treatment obviously decreased the p-TAK1 and t-TAK1 levels (*Figure* 7B), and HE staining showed that AAV-shRNA-TAK1 significantly decreased inflammation (*Figure* 7C and 7D). We also examined fibrosis and atrophy after AAV-shRNA-TAK1 treatment and observed obvious reductions in α-SMA and MuRF1 expression and an increase in MHC expression, in the AAV-shRNA-TAK1-treated mdx mice (*Figure* 7E). These anti-fibrotic and anti-atrophic effects of AAV-shRNA-TAK1 were also observed in DIA muscle (*Figure* 7F). The anti-fibrotic effect was confirmed via fibronectin immunofluorescence staining (*Figure* 7G and 7H) and the hydroxyproline assay of the TA and DIA sections (*Figure* S5E). DMD atrophy is partly due to the inhibition of differentiation; we measured myoblast determination protein 1 (MyoD), myogenin, and myostatin levels in TA and DIA muscles and found increased protein levels of all three substances in AAV-shRNA-control mdx mice. In contrast, the AAV-shTAK1 group showed

DOI: 10.1002/jcsm.12650

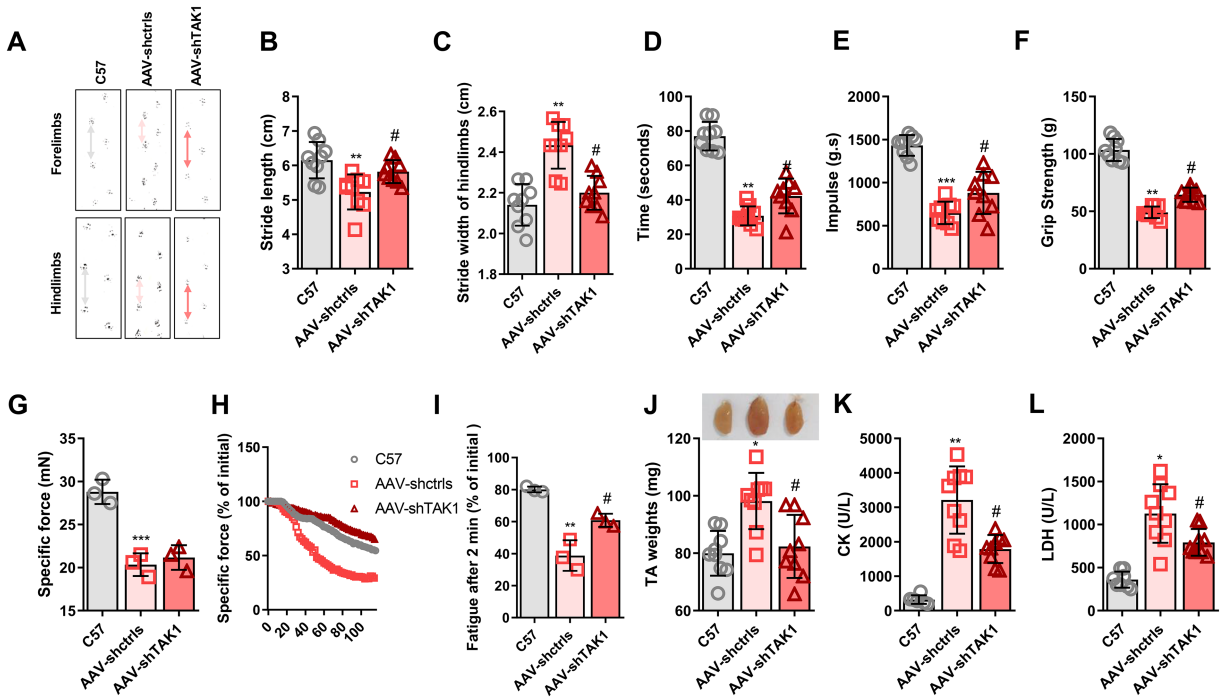

Figure 6 TAK1 knockdown improves muscle function and increases TA muscle force in mdx mice. (A) Representative images of gait tracking after tail injection of AAV-2/9-shRNA-TAK1 for 4 weeks and quantification of (B) stride length and (C) stride width of hindlimbs (n = 9). (D) The length of time until the mice fell from the wire was recorded and (E) the physical impulse was calculated to take into account the smaller body weight of control mice and mdx mice (n = 9). (F) In vivo muscle strength was evaluated by measuring the forelimb grip strength using a calibrated grip strength tester (n = 9). (G) Representative traces of TA force for all mice during 2 min of fatiguing contractions and (H) the pooled values of TA force after 1 min of fatigue (n = 3). (I) Pooled values of TA force recovery after fatigue from 2 to 10 min (n = 3). (J) TA weights were measured after injection of AAV-shRNA-TAK1 in mdx mice for 4 weeks (n = 9). (L) Serum CK and (L) LDH activity (n = 9). Values are expressed as means ± standard deviation (SD), $*P < 0.05$, $***P < 0.001$ vs. control group; $\#P < 0.05$ vs. AAV-shctrls. AAV, adeno-associated virus; CK, creatine kinase; LDH, lactic dehydrogenase; TA, tibialis anterior.

decreased myostatin, but not MyoD or myogenin, expression (*Figure* S5F and S5G), while the DIA muscles of AAV-shRNA-control mdx mice exhibited decreased MyoD and myogenin expression, but increased myostatin expression. Only myostatin showed decreased expression in the AAV-shTAK1 group (*Figure* S5H and S5I). In addition, the TA muscles of AAV-shRNA-control mdx mice exhibited reduced MHC, and increased eMyHC, expression compared with controls; these changes were reversed by AAV-shRNA-TAK1 treatment (*Figure* 7I). Moreover, eMyHC was virtually absent from the DIA muscles of the AAV-control group, in which a robust reduction of MHC expression was also seen; in contrast, AAV-shRNA-TAK1 treatment increased MHC expression in the DIA muscles (*Figure* 7J).

NG25 improves myoblast differentiation and alleviates fibrosis in mdx mice

NG25 is a common TAK1 inhibitor that binds to the ATP binding pocket of residues 184–187 in the target kinase. Many studies have reported that NG25 can inhibit TAK1 phosphorylation.[30,31] Therefore, we investigated the therapeutic effects of NG25 on a mouse model of DMD (Supporting Information, *Figure* S6A). After treatment with NG25 for 2 weeks, all mice were subjected to gait analysis according to a previously published procedure.[17] Stride length and forelimb stride width were both reduced, while hindlimb stride width was increased, compared with control mice; these changes were reversed by NG25 treatment (*Figure* 8A–8D). Furthermore, NG25 treatment partially restored muscle function, as evidenced by the 48% increase in maximum grip strength (*Figure* 8E). Also, NG25 attenuated the significantly increased serum CK and LDH levels seen in the mdx mice (*Figure* 8F and 8G). Finally, hypertrophy of the TA muscle was partially reduced by NG25 treatment (*Figure* S6B and S6C). In summary, NG25 improved muscle quality and performance in mdx mice.

NG25 treatment had no effect on IL-1β, TNF-α, or TGF-β1 levels, as shown by both reverse transcription-quantitative PCR and ELISA analyses (*Figure* S6D–S6G). In TA muscle, a significant reduction of p-TAK1 was seen in the NG25 treatment group (*Figure* 9A); DIA muscle p-TAK1 levels were also markedly decreased by NG25 treatment (*Figure* 9B). Histological

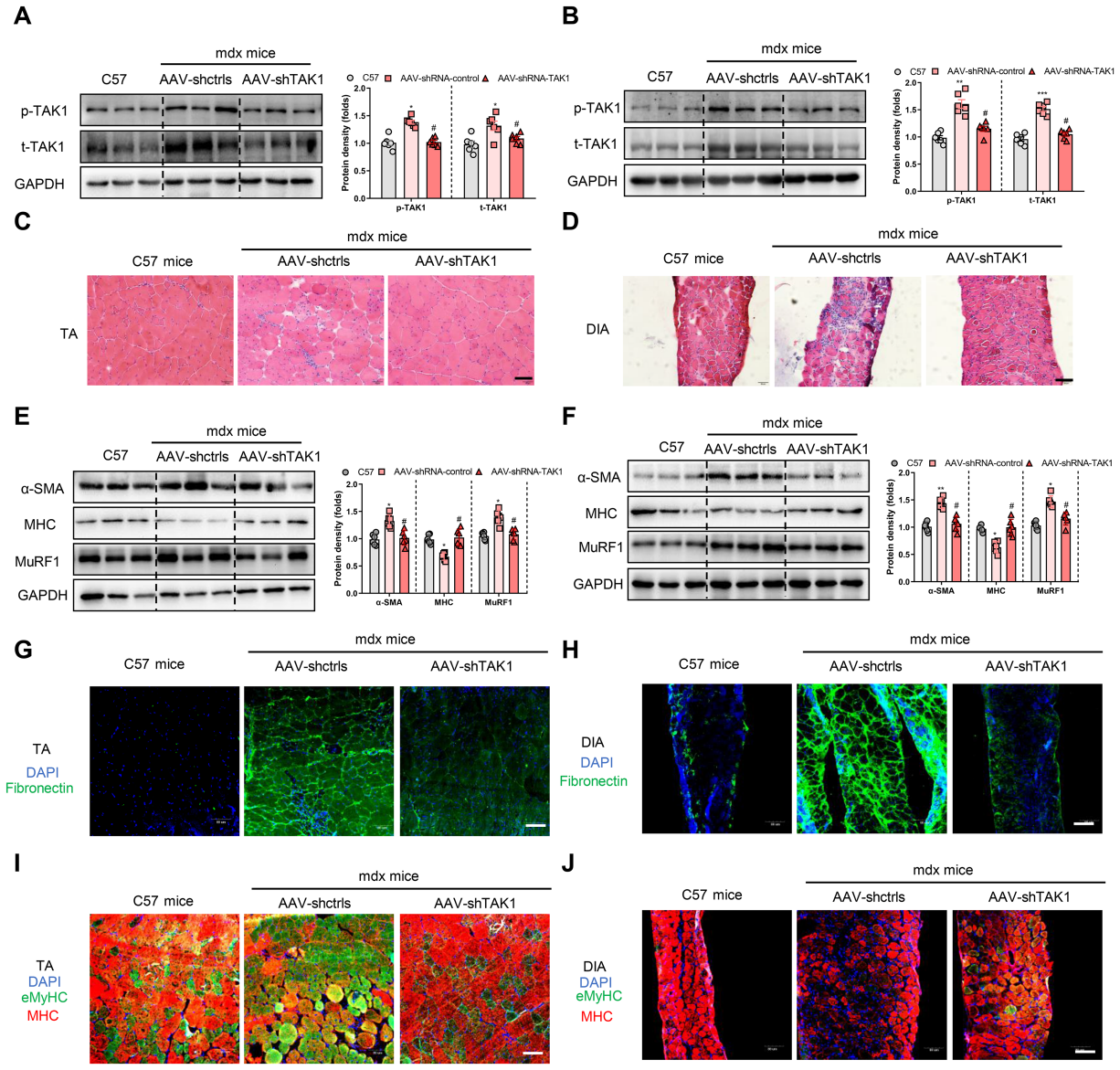

Figure 7 TAK1 knockdown regulates myoblasts differentiation and controls fibrosis in mdx mice. (A) Western blot of p-TAK1 (Thr-184/187), t-TAK1 protein levels in TA of mdx mice. (B) Western blot of p-TAK1 (Thr-184/187), t-TAK1 protein levels in DIA of mdx mice. (C) Representative HE stained images of TA and (D) DIA sections. Scale bar, 100 μm. (E) Western blot of α-SMA, MHC, and MuRF1 protein levels in TA of mdx mice. (F) Western blot of α-SMA, MHC, and MuRF1 protein levels in DIA of mdx mice. (G) Fluorescent fibronectin-stained TA and (H) DIA sections. Scale bar, 100 μm. (I) Fluorescent MHC (red) and eMyHC (green)-stained TA (upper panel) and (J) DIA sections, and nuclei are stained with DAPI (blue). Scale bar, 100 μm. Values are expressed as means ± standard deviation (SD) (n = 6), $^{*}P < 0.05$, $^{**}P < 0.01$, $^{***}P < 0.001$ vs. control group; $\#P < 0.05$, $\#\#P < 0.01$, $\#\#\#P < 0.001$ vs. AAV-shctrls. α-SMA, alpha-smooth muscle actin; AAV, adeno-associated virus; DAPI, 4′,6-diamidino-2-phenylindole; DIA, diaphragm; GAPDH, glyceraldehyde 3-phosphate dehydrogenase; MHC, myosin heavy chain; MuRF1, muscle RING-finger 1; p-TAK1, phosphorylated transforming growth factor-β-activated kinase 1; t-TAK1, total transforming growth factor-β-activated kinase 1; TA, tibialis anterior.

assessment of the TA and DIA muscles revealed less inflammation in NG25-treated mdx mice compared with controls (*Figure* 9C and 9D). Next, we examined fibrosis and atrophy after NG25 treatment and noted a marked reduction in α-SMA and MuRF1 protein levels and an increase in MHC expression (*Figure* 9E) in NG25-treated mdx mice. Moreover, these anti-fibrotic and anti-atrophic effects of NG25 were observed in the DIA muscles (*Figure* 9F). The anti-fibrotic effect of NG25 was confirmed via fibronectin immunofluorescence staining (*Figure* 9G and 9H) and the hydroxyproline assay of the TA and DIA sections (*Figure* S6H). We then measured MyoD, myogenin, and myostatin levels in the TA and DIA muscles; mdx mice showed an increase in the protein levels of MyoD, myogenin, and myostatin only for TA muscle.

DOI: 10.1002/jcsm.12650

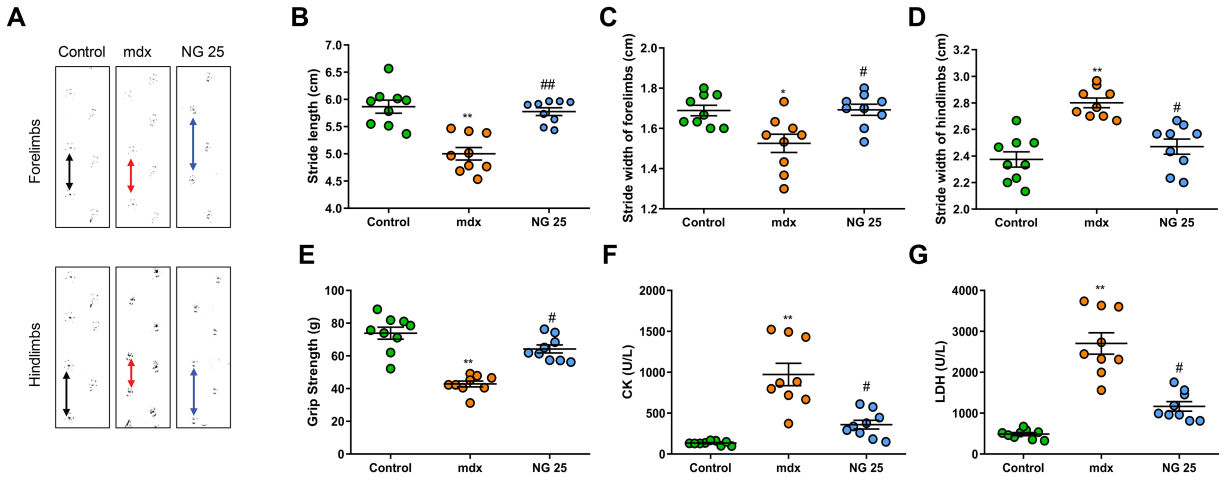

Figure 8 NG25 treatment in mdx mice improves muscle function and minimizes muscle damage. (A) Representative images of gait tracking and quantification of (B) stride length, (C) stride width of hindlimbs, and (D) stride width of forelimbs (n = 9). (E) In vivo muscle strength was evaluated by measuring the forelimb grip strength using a calibrated grip strength tester (n = 9). (F) Serum CK and (G) LDH activity (n = 9). Values are expressed as means ± standard deviation (SD), *$P < 0.05$, ***$P < 0.001$ vs. control group; #$P < 0.05$ vs. mdx mice. CK, creatine kinase; LDH, lactic dehydrogenase.

By contrast, myostatin expression was decreased in the NG25 treatment group (*Figure* S6I and S6J). The DIA muscles of mdx mice exhibited decreased MyoD and myogenin expression levels, but an increased myostatin level; in the NG25 treatment group, only myostatin showed decreased expression (*Figure* S6K and S6L). The TA muscle sections of mdx mice showed lower MHC, and higher eMyHC, expression compared with controls; these changes were reversed by NG25 treatment (*Figure* 9I). Finally, eMyHC was virtually absent from the DIA muscles of mdx mice, and a robust reduction in MHC expression was also seen. In contrast, NG25 treatment increased DIA muscle MHC expression (*Figure* 9J).

Discussion

Duchenne muscular dystrophy is a rare, degenerative, and fatal muscle disease characterized by muscle wasting and fibrosis, which are the major causes of death among sufferers of this disorder.[32] In this study, we identified a new anti-fibrotic and anti-atrophic treatment approach for DMD involving the inhibition of TAK1. Cytokines were secreted after muscle injury. These inflammatory cytokines activate TAK1 through various pathways, as reported previously,[33,34] which may inhibit myoblast differentiation and induce fibrosis (*Figure* 10). TAK1 has been shown to be vital in the transdifferentiation of myoblasts into fibroblasts; we show here that inhibition of TAK1 could both promote myoblast differentiation and attenuate fibrosis by preventing transdifferentiation, thus improving dystrophic muscle function.

The mdx mouse strain is widely used to study DMD. In this study, the mouse model used is not the regular mdx with a point mutation in exon 23, and we used another dystrophic model with the specifics of the mutation in exon 4. We found that the mdx mice and DMD patients exhibit many biochemical and histological similarities. One study found that DMD patients exhibited extensive and severe muscle fibrosis, and mdx mice high-level fibrosis, principally in the DIA muscles.[35] Therefore, we evaluated fibrosis in DIA muscle tissues. The TA muscle of mdx mice is characterized by necrosis accompanied by persistent and progressive degeneration, although this is offset by a regenerative process catalyzed by satellite cells.[36] Another study found that differentiation of regenerated myotubes into new types of fibres was significantly inhibited in the TA muscle of mdx mice.[37] Thus, we focused on the TA muscle when exploring myoblast differentiation.

The inflammatory cytokines responsible for muscle damage remain subject to debate.[38,39] Some studies have shown that inflammatory cytokines initiate profibrotic reactions, in turn promoting the activation of fibroblasts and inducing collagen I and fibronectin production.[40,41] Thus, anti-inflammatory agents remain important as a therapeutic tool for DMD and related neuromuscular diseases. However, other studies have shown that, following skeletal muscle injury, inflammatory cytokines are required for muscle regeneration via the activation of muscle satellite cells.[42,43] Thus, inflammatory cytokines play an important role in muscle repair after injury. We observed a significant increase in inflammatory cytokines in mdx mice compared with controls, as also reported previously.[44] To control the profibrotic reaction induced by inflammatory cytokines while also allowing for muscle regeneration, inflammatory cytokines were not cleared away directly in our experiments. We found that, in primary myoblasts from both DMD patients and mdx mice, TAK1 was activated by TGF-β1, IL-1β, and TNF-α (*Figure* 3). In this study, TAK1 is not only affecting myoblasts but

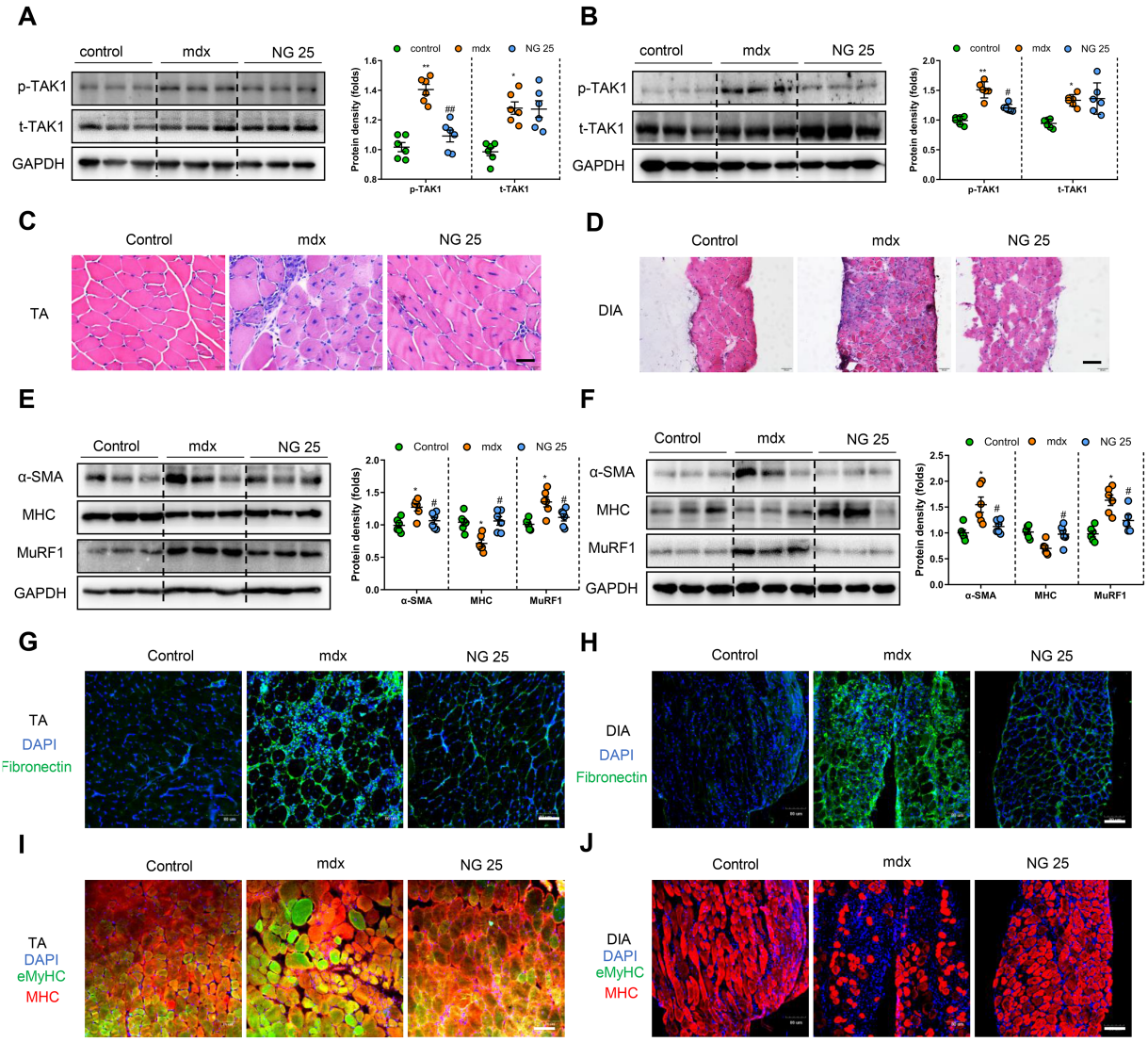

Figure 9 NG25 treatment in mdx mice regulates myoblasts differentiation and controls fibrosis in mdx mice. NG25 treatment in mdx mice for 2 weeks. (A) Western blot of p-TAK1 (Thr-184/187), t-TAK1 protein levels in TA of mdx mice. (B) Western blot of p-TAK1 (Thr-184/187), t-TAK1 protein levels in DIA of mdx mice. (C) Representative HE stained images of TA and (D) DIA sections. Scale bar, 100 μm. (E) Western blot of α-SMA, MHC, and MuRF1 protein levels in TA of mdx mice. (F) Western blot of α-SMA, MHC, and MuRF1 protein levels in DIA of mdx mice. (G) Fluorescent fibronectin-stained TA and (H) DIA sections of mdx mice. Scale bar, 100 μm. (I) Fluorescent MHC (red) and eMyHC (green)-stained TA and (J) DIA sections of mdx mice, and nuclei are stained with DAPI (blue). Scale bar, 100 μm. Values are expressed as means ± standard deviation (SD) (n = 6), *$P < 0.05$, **$P < 0.01$, ***$P < 0.001$ vs. control group; #$P < 0.05$, ##$P < 0.01$, ###$P < 0.001$ vs. mdx mice. α-SMA, alpha-smooth muscle actin; AAV, adeno-associated virus; DAPI, 4′,6-diamidino-2-phenylindole; DIA, diaphragm; eMyHC, embryonic myosin heavy chain; GAPDH, glyceraldehyde 3-phosphate dehydrogenase; MHC, myosin heavy chain; MuRF1, muscle RING-finger 1; p-TAK1, phosphorylated transforming growth factor-β-activated kinase 1; t-TAK1, total transforming growth factor-β-activated kinase 1; TA, tibialis anterior.

potentially myofibres a well (Supporting Information, *Figure* S7A). Early reports showed that TAK1 activation induced and maintained fibrosis in many fibrosis-associated diseases,[45,46] and we found that TAK1 activation promoted fibrosis and atrophy of skeletal muscle in mdx mice (*Figure* 5). Conversely, TAK1 inhibition improved myoblast differentiation and alleviated fibrosis, in turn improving skeletal muscle function. Inhibition of TGF-β1 reportedly conferred a protective effect against DMD[11]; in this study, TAK1 was activated by IL-1β, TNF-α, and TGF-β1. For DMD, the therapeutic effect of TAK1 inhibition may be stronger than that of TGF-β1 inhibition; we will investigate this more thoroughly in further studies.

TAK1 plays an important role in satellite cell homeostasis and function. Recent studies have shown that TAK1 regulates skeletal muscle mass and mitochondrial function,[47] and knockout of TAK1 in muscle resulted in the accumulation of oxidative stress and dysfunction in the regeneration

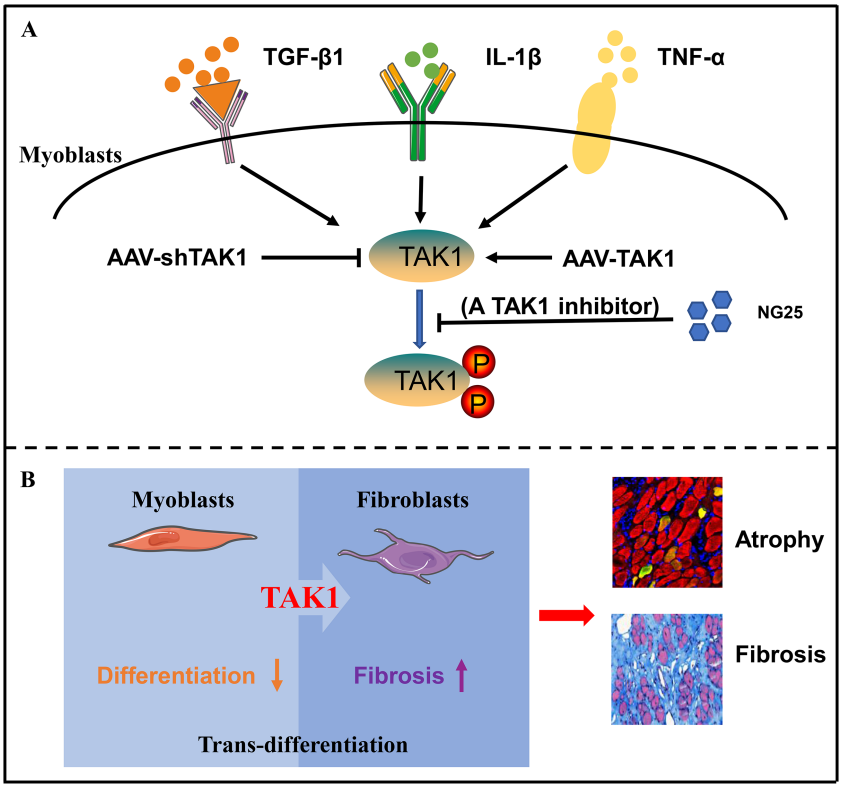

Figure 10 Schematic diagram depicting the possible mechanism in DMD by inhibition of TAK1 in skeletal muscle. (A) TGF-β1, IL-1β, and TNF-α are secreted by immune cells in dystrophic muscle following acute injury, which result in TAK1 phosphorylation. TAK1 phosphorylation aggravates muscle fibrosis and muscle degeneration in DMD. TAK1 knockdown by AAV-shRNA or NG25 improves the dystrophic muscle function by competitive binding with TAK1 to avoid overphosphorylation of TAK1, (B) which subsequently results in reduced fibrosis and enhancement of myoblasts differentiation. AAV, adeno-associated virus; IL, interleukin; TAK1, transforming growth factor-β-activated kinase 1; TNF-α, tumour necrosis factor-α.

response following muscle injury.[48] Therefore, we did not perform the experiment with TAK1 global heterozygous mice or skeletal muscle-specific TAK1 knockout mice. In this study, TAK1 was overexpressed in DMD patients and mdx mice. TAK1 activation caused fibrosis and muscle wasting in control mice, and TAK1 overexpression further aggravated muscle fibrosis and exacerbated muscle wasting in mdx mice (*Figure* 5). Moreover, TAK1 activation inhibited myoblast differentiation and promoted collagen I production in primary myoblasts from mdx mice. Therefore, we suggest that muscle wasting and fibrosis in DMD are attributable to TAK1 activation by cytokines. Most importantly, we found that inhibition of TAK1 by AAV-shRNA or NG25 improved myoblast differentiation and alleviated fibrosis in mdx mice. In this study, we found that TAK1 activation induced transdifferentiation of myoblasts. TAK1 inhibition partly suppressed transdifferentiation of myoblasts from mdx mice. Thus, we suppose that TAK1 activation may also induce the transdifferentiation of fibro-adipogenic progenitor cells in mdx mice. We will further explore the role of TAK1 activation on the transdifferentiation of fibro-adipogenic progenitor cells in the next study.

A recent study reported that TGF-β1 induced the transdifferentiation of myoblasts into fibroblasts.[49] Similarly, in our previous study, TAK1 activation induced transdifferentiation of myoblasts into fibroblasts.[50] In addition, TAK1 was activated by TGF-β1, IL-1β, and TNF-α in this study. Although our study indicates that TAK1 activation inhibits myoblast differentiation and increases myoblast transdifferentiation, in turn promoting muscle wasting and fibrosis, further studies should investigate the detailed mechanism underlying TAK1-induced transdifferentiation of myoblasts. To specifically knock down TAK1 in skeletal muscles, the AAV-shRNA-control and AAV-shRNA-TAK1 were intramuscularly injected into the right and left TA muscles, respectively, of mdx and control mice. We found that TAK1 inhibition improved myoblast differentiation and alleviated fibrosis in mdx mice.[50] In addition, we found that p38-MAPK and MAP 4K2 were activated in the skeletal muscle of mdx mice, while AAV-shTAK1 and NG25 did not affect MAP 4K2 expression in mdx mice (*Figure* S7B and S7C). Therefore, the beneficial mechanism of AAV-shTAK1 and NG25 is independent of p38-MAPK/MAP 4K2 pathway. In the future, we will explore the pathway downstream of

TAK1 in more detail, with the aim of improving its beneficial effects on myoblast differentiation and fibrosis.

In conclusion, this study provides evidence that TGF-β1, IL-1β, and TNF-α are secreted in dystrophic muscles following acute injury, which promotes TAK1 activation (*Figure* 10). TAK1 activation exacerbates fibrosis and muscle degeneration, and pharmacological inhibition of TAK1 could improve the condition of dystrophic muscles by reducing fibrosis and increasing myoblast differentiation and muscle strength.

Author contributions

Dengqiu Xu, Lu Wang, and Sijia Li researched the data, contributed to discussions, and wrote the manuscript. Xihua Li and Lei Zhao collected and analysed clinical data. Zeren Sun, Xiaofei Huang, and Chunjie Li collected and analysed data. Lixin Sun reviewed the manuscript. Zhenzhou Jiang conceived the experiments, researched the data, and edited/reviewed the manuscript. Luyong Zhang is the guarantor of this work and had full access to all the data in the study and takes responsibility for the integrity of the data and the accuracy of the data analysis.

Acknowledgements

This work was supported by the grants from the Scholar of the 14th Batch of 'Six Talents Peak' High-level Talent Selection programme (SWYY-094); the Postgraduate Research Practice Innovation Program of Jiangsu Province (KYCX19-0763); the 'Double First-Class' University project (CPU2018GY33); the National Natural Science Foundation of China (81773827, 81573514), to J.Z.; the National Natural Science Foundation of China (81773995), to Z.L.; and the National Natural Science Foundation of China (81873084, 81573690), to S.L.

The authors certify that they comply with the ethical guidelines for authorship and publishing of the *Journal of Cachexia, Sarcopenia and Muscle*.[51] The clinical study was approved by the Institutional Review Board at Children's Hospital of Fudan University, and all participants provided written informed consent prior to initiation of study procedures. This study is registered clinical trial at Children's Hospital of Fudan University (NCT number: 2019-244). All experimental procedures performed on the mice were conducted in accordance with the guidelines of the Institutional Animal Care and Use Committee of China Pharmaceutical University (Nanjing, China; 2019-11-006), and the use of the laboratory animals was approved by the Laboratory Animal Management Committee Office (Nanjing, China).

Online supplementary material

Additional supporting information may be found online in the Supporting Information section at the end of the article.

Table S1. The primers used for Real-time quantitative PCR (house mouse)
Table S2. The antibody used for Western blot analysis

Figure S1 Fibrosis in and atrophy of the muscles of DMD patients is accompanied by TAK1 activation. (A) Fluorescent dystrophin (green)-stained triceps sections of controls and DMD patients. (B) Serum CK levels were used to examine the whole-body muscles health. (C) Representative H&E stained images of triceps sections. (D and E) Western blot of Murf1 protein level in triceps of controls and DMD patients. (F) Fluorescent TGF-β1 (green)-stained triceps sections of controls and DMD patients. Scale bar, 100 μm. (G) Western blot of TGF-β1 protein level. Values are expressed as means ± standard deviation (SD) (n = 6), $^{**}p < 0.01$, $^{***}p < 0.001$ vs. control.

Figure S2 TAK1 was activated in mouse primary myoblasts by IL-1β, TNF-α and TGF-β1. (A-C) Serum IL-1β, TNF-α and TGF-β1 level for 6 weeks aged control and mdx mice. Values are expressed as means ± standard deviation (SD) (n = 12), $^{**}p < 0.01$, $^{***}p < 0.001$ vs. control mice (CON). (D and E) Primary myoblasts isolated from EDL muscle of mdx mice, then myoblasts treated with 0, 1, 2, 5 10 and 20 ng/ml IL-1β or TNF-α or TGF-β1 for 2 hours. Western blot of p-TAK1 and t-TAK1 protein levels and the pooled values for each group. Values are expressed as means ± standard deviation (SD) (n = 6), $^{*}p < 0.05$, $^{**}p < 0.01$, $^{***}p < 0.001$ vs. control group.

Figure S3 TAK1 regulated myoblasts differentiation and fibrosis in primary myoblasts. Primary myoblasts from EDL muscle of mdx mice, then myoblasts treated with TGF-β1 (0, 1, 2.5 and 5 ng/ml) for 48 hours. (A and B) Western blot of MyoD, myogenin and myostatin protein levels and the pooled values for each group (n = 3). (C and D) Western blot of MuRF1, MHC and Collagen I protein levels (n = 3). $^{*}p < 0.05$, $^{**}p < 0.01$ vs. control group (0 ng/ml TGF-β1).

Figure S4 TAK1 activation exacerbated muscle damage in mdx mice. (A-C) Western blot of p-TAK1 and t-TAK1 protein levels in TA. (D-F) Western blot of p-TAK1and t-TAK1 protein levels in DIA (n = 3). (G) Representative H&E stained images of (upper panel) TA and (lower panel) DIA sections (n = 6). Values are expressed as means ± standard devia-

tion (SD), **p < 0.01, ***p < 0.001 vs. control group; #p < 0.05, ##p < 0.01, ###p < 0.001 vs. AAV-ctrls.

Figure S5 TAK1 knockdown improved muscle function in mdx mice. (A) Schematic diagram of animal experiment design. Knockdown TAK1 protein expression was performed by tail injection of AAV-shRNA-TAK1 in mdx mice. (B) In vivo fluorescence imaging using the IVIS Spectrum system. (C) Representative images of green fluorescent protein (GFP) in TA section. (D) Serum IL-1β, TNF-α and TGF-β1 levels were measured by using enzyme-linked immunosorbent assay kits, respectively. (E) Hydroxyproline content (μg hydroxyproline/mg muscle) in TA and DIA muscles. Values are expressed as means ± standard deviation (SD) (n = 6), *p < 0.05, ***p < 0.001 vs. control group; #p < 0.05 vs. AAV-shctrls.

Figure S6 NG25 treatment in mdx mice minimized muscle damage. (A) Schematic diagram of animal experiment design. NG25 treatment in mdx mice for 2 weeks. (B) Representative images of TA in each group and (C) TA weights were measured after NG25 treatment for 2 weeks (n = 9). (D) The relative mRNA levels of IL-1β, TNF-α and TGF-β1 measured by RT-qPCR (n = 6). (E-G) Serum IL-1β, TNF-α and TGF-β1 levels were measured by using enzyme-linked immunosorbent assay kits, respectively (n = 8). (H) Hydroxyproline content (μg hydroxyproline/mg muscle) in TA and DIA muscles (n = 6). Values are expressed as means ± standard deviation (SD) (n = 6), *p < 0.05, ***p < 0.001 vs. control group; #p < 0.05 vs. mdx mice.

Figure S7 The beneficial mechanism of AAV-shTAK1 and NG25 on DMD is independent of p38-MAPK/MAP 4 K2 pathway. (A) Fluorescent p-TAK1 (green)-stained TA sections of controls and mdx mice, and nuclei are stained with DAPI (blue). Scale bar, 100 μm. (B and C) Western blot of p-p38 MAPK, t-p38 MAPK and MAP 4 K2 protein levels in triceps of controls and mdx mice.

Conflict of interest

The authors declare that there are no conflicts of interest.

References

1. Mendell JR, Shilling C, Leslie ND, Flanigan KM, al-Dahhak R, Gastier-Foster J, et al. Evidence-based path to newborn screening for Duchenne muscular dystrophy. *Ann Neurol* 2012;**71**:304–313.
2. McGreevy JW, Hakim CH, McIntosh MA, Duan DS. Animal models of Duchenne muscular dystrophy: from basic mechanisms to gene therapy. *Dis Model Mech* 2015;**8**:195–213.
3. Chamberlain JR, Chamberlain JS. Progress toward gene therapy for Duchenne muscular dystrophy. *Mol Ther* 2017;**25**:1125–1131.
4. Walcher T, Steinbach P, Spiess J, Kunze M, Gradinger R, Walcher D, et al. Detection of long-term progression of myocardial fibrosis in Duchenne muscular dystrophy in an affected family: a cardiovascular magnetic resonance study. *Eur J Radiol* 2011;**80**:115–119.
5. Farini A, Gowran A, Bella P, Sitzia C, Scopece A, Castiglioni E, et al. Fibrosis rescue improves cardiac function in dystrophin-deficient mice and Duchenne patient-specific cardiomyocytes by immunoproteasome modulation. *Am J Pathol* 2019;**189**:339–353.
6. Kawano R, Ishizaki M, Maeda Y, Uchida Y, Kimura E, Uchino M. Transduction of full-length dystrophin to multiple skeletal muscles improves motor performance and life span in utrophin/dystrophin double knockout mice. *Mol Ther* 2008;**16**:825–831.
7. Haslett JN, Sanoudou D, Kho AT, Bennett RR, Greenberg SA, Kohane IS, et al. Gene expression comparison of biopsies from Duchenne muscular dystrophy (DMD) and normal skeletal muscle. *Proc Natl Acad Sci U S A* 2002;**99**:15000–15005.
8. Pessina P, Cabrera D, Morales MG, Riquelme CA, Gutierrez J, Serrano AL, et al. Novel and optimized strategies for inducing fibrosis in vivo: focus on Duchenne muscular dystrophy. *Skeletal Muscle* 2014;**4**:2952–2962.
9. Malecova B, Gatto S, Etxaniz U, Passafaro M, Cortez A, Nicoletti C, et al. Dynamics of cellular states of fibro-adipogenic progenitors during myogenesis and muscular dystrophy. *Nat Commun* 2018;**9**:3670.
10. Yen TNF, Aardal NP, Bronner MP, Thorning DR, Savard CE, Lee SP, et al. Myofibroblasts are responsible for the desmoplastic reaction surrounding human pancreatic carcinomas. *Surgery* 2002;**131**:129–134.
11. Taniguti APT, Pertille A, Matsumura CY, Neto HS, Marques MJ. Prevention of muscle fibrosis and myonecrosis in mdx mice by suramin, a TGF-beta 1 blocker. *Muscle Nerve* 2011;**43**:82–87.
12. Feder D, Rugollini M, Santomauro A, Oliveira LP, Lioi VP, dos Santos R, et al. Erythropoietin reduces the expression of myostatin in mdx dystrophic mice. *Brazilian J Med Biol Res* 2014;**47**:966–971.
13. Gieseck RL, Wilson MS, Wynn TA. Type 2 immunity in tissue repair and fibrosis. *Nat Rev Immunol* 2018;**18**:62–76.
14. Brown K, Vial SCM, Dedi N, Long JM, Dunster NJ, Cheetham GMT. Structural basis for the interaction of TAK1 kinase with its activating protein TAB1. *J Mol Biol* 2005;**354**:1013–1020.
15. Il Kim S, Kwak JH, Zachariah M, He YJ, Wang L, Choi ME. TGF-beta-activated kinase 1 and TAK1-binding protein 1 cooperate to mediate TGF-beta(1)-induced MKK3-p38 MAPK activation and stimulation of type I collagen. *Am J Physiol-Renal Physiol* 2007;**292**:F1471–F1478.
16. Richardson L, Dixon CL, Aguilera-Aguirre L, Menon R. Oxidative stress-induced TGF-beta/TAB1-mediated p38MAPK activation in human amnion epithelial cells. *Biol Reprod* 2018;**99**:1100–1112.
17. Milad N, White Z, Tehrani AY, Sellers S, Rossi FMV, Bernatchez P. Increased plasma lipid levels exacerbate muscle pathology in the mdx mouse model of Duchenne muscular dystrophy. *Skeletal Muscle.* 2017;**7**:19–27.
18. Xu DQ, Jiang ZZ, Sun ZR, Wang L, Zhao GL, Hassan HM, et al. Mitochondrial dysfunction and inhibition of myoblast differentiation in mice with high-fat-diet-induced pre-diabetes. *J Cell Physiol* 2019;**234**:7510–7523.
19. Percival JM, Whitehead NP, Adams ME, Adamo CM, Beavo JA, Froehner SC. Sildenafil reduces respiratory muscle weakness and fibrosis in the mdx mouse model of Duchenne muscular dystrophy. *J Pathol* 2012;**228**:77–87.
20. Xu DQ, Wang L, Jiang ZZ, Zhao GL, Hassan HM, Sun LX, et al. A new hypoglycemic mechanism of catalpol revealed by enhancing MyoD/MyoG-mediated myogenesis. *Life Sci* 2018;**209**:313–323.
21. Wang L, Xu DQ, Li LP, Xing X, Liu L, Abdelmotalab MI, et al. Possible role of

hepatic macrophage recruitment and activation in triptolide-induced hepatotoxicity. *Toxicol Lett* 2018;**299**:32–39.
22. Whitehead NP, Kim MJ, Bible KL, Adams ME, Froehner SC. A new therapeutic effect of simvastatin revealed by functional improvement in muscular dystrophy. *Proc Natl Acad Sci U S A* 2015;**112**:12864–128659.
23. Zanotti S, Bragato C, Zucchella A, Maggi L, Mantegazza R, Morandi L, et al. Anti-fibrotic effect of pirfenidone in muscle derived-fibroblasts from Duchenne muscular dystrophy patients. *Life Sci* 2016;**145**:127–136.
24. Bowen TS, Adams V, Werner S, Fischer T, Vinke P, Brogger MN, et al. Small-molecule inhibition of MuRF1 attenuates skeletal muscle atrophy and dysfunction in cardiac cachexia. *J Cachexia Sarcopenia Muscle* 2017;**8**:939–953.
25. Dubash AD, Kam CY, Aguado BA, Patel DM, Delmar M, Shea LD, et al. Plakophilin-2 loss promotes TGF-beta 1/p38 MAPK-dependent fibrotic gene expression in cardiomyocytes. *J Cell Biol* 2016;**212**:425–438.
26. Li J, Liang C, Zhang ZK, Pan XH, Peng SL, Lee WS, et al. TAK1 inhibition attenuates both inflammation and fibrosis in experimental pneumoconiosis. *Cell Discov* 2017;**3**:21–41.
27. van Putten M, Kumar D, Hulsker M, Hoogaars WMH, Plomp JJ, van Opstal A, et al. Comparison of skeletal muscle pathology and motor function of dystrophin and utrophin deficient mouse strains. *Neuromuscul Disord* 2012;**22**:406–417.
28. Xie J, Tu T, Zhou SH, Liu QM. Transforming growth factor (TGF)-beta 1 signal pathway: a promising therapeutic target for attenuating cardiac fibrosis. *Int J Cardiol* 2017;**239**:9.
29. Vetrone SA, Montecino-Rodriguez E, Kudryashova E, Kramerova I, Hoffman EP, Liu SD, et al. Osteopontin promotes fibrosis in dystrophic mouse muscle by modulating immune cell subsets and intramuscular TGF-beta. *J Clin Invest* 2009;**119**:1583–1594.
30. Tan L, Nomanbhoy T, Gurbani D, Patricelli M, Hunter J, Geng J, et al. Discovery of type II inhibitors of TGF beta-activated kinase 1 (TAK1) and mitogen-activated protein kinase kinase kinase kinase 2 (MAP 4K2). *J Med Chem* 2015;**58**:183–196.
31. Wang H, Chen Z, Li Y, Ji QY. NG25, an inhibitor of transforming growth factor-activated kinase 1, ameliorates neuronal apoptosis in neonatal hypoxic-ischemic rats. *Mol Med Rep* 2018;**17**:1710–1716.
32. Crone M, Mah JK. Current and emerging therapies for Duchenne muscular dystrophy. *Curr Treat Options Neurol* 2018;**20**:17–31.
33. Liao SJ, Luo J, Li D, Zhou YH, Yan B, Wei JJ, et al. TGF-beta 1 and TNF-alpha synergistically induce epithelial to mesenchymal transition of breast cancer cells by enhancing TAK1 activation. *J Cell Commun Signal* 2019;**13**:369–380.
34. Lei CQ, Wu X, Zhong X, Jiang L, Zhong B, Shu HB. USP19 inhibits TNF-alpha- and IL-1 beta-triggered NF-kappa B activation by deubiquitinating TAK1. *J Immunol* 2019;**203**:259–268.
35. Muller J, Vayssiere N, Royuela M, Leger ME, Muller A, Bacou F, et al. Comparative evolution of muscular dystrophy in diaphragm, gastrocnemius and masseter muscles from old male mdx mice. *J Muscle Res Cell Motil* 2001;**22**:133–139.
36. Yuasa K, Hagiwara Y, Ando M, Nakamura A, Takeda S, Hijikata T. MicroRNA-206 is highly expressed in newly formed muscle fibers: implications regarding potential for muscle regeneration and maturation in muscular dystrophy. *Cell Struct Funct* 2008;**33**:163–169.
37. Ngoc LN, Ferry A, Schnell FJ, Hanson GJ, Popplewell L, Dickson G, et al. Functional muscle recovery following dystrophin and myostatin exon splice modulation in aged mdx mice. *Hum Mol Genet* 2019;**28**:3091–3100.
38. Minari ALA, Avila F, Oyama LM, Thomatieli-Santos RV. Skeletal muscle induce recruitment of Ly6C + macrophages subtype and release inflammatory cytokines 3 days after downhill exercise. *Am J Physiol Regul Integr Comp Physiol* 2019;**4**:R597–R605.
39. Qazi TH, Duda GN, Ort MJ, Carsten P, Sven G, Tobias W. Cell therapy to improve regeneration of skeletal muscle injuries. *J Cachexia Sarcopenia Muscle* 2019;**10**:501–516.
40. Liu XG, Zeng ZG, Zhao LL, Xiao WH, Chen PJ. Changes in inflammatory and oxidative stress factors and the protein synthesis pathway in injured skeletal muscle after contusion. *Exp Ther Med* 2018;**15**:2196–2202.
41. Scheibe K, Kersten C, Schmied A, Vieth M, Primbs T, Carle B, et al. Inhibiting interleukin 36 receptor signaling reduces fibrosis in mice with chronic intestinal inflammation. *Gastroenterology* 2019;**156**:1082–1097.
42. Kim J, Lee J. Role of transforming growth factor-beta in muscle damage and regeneration: focused on eccentric muscle contraction. *J Exerc Rehab* 2017;**13**:621–626.
43. Novak JS, Hogarth MW, Boehler JF, Nearing M, Vila MC, Heredia R, et al. Myoblasts and macrophages are required for therapeutic morpholino antisense oligonucleotide delivery to dystrophic muscle. *Nat Commun* 2017;**8**:941–953.
44. Serra F, Quarta M, Canato M, Toniolo L, de Arcangelis V, Trotta A, et al. Inflammation in muscular dystrophy and the beneficial effects of non-steroidal anti-inflammatory drugs. *Muscle Nerve* 2012;**46**:773–784.
45. Ma FY, Tesch GH, Ozols E, Xie M, Schneider MD, Nikolic-Paterson DJ. TAK1 regulates pro-inflammatory and pro-fibrotic responses in tubular epithelial cells. *Nephrol Ther* 2009;**14**:A33–A33.
46. Zhou J, Zhong JY, Huang ZX, Liao MJ, Lin S, Chen J, et al. TAK1 mediates apoptosis via p38 involve in ischemia-induced renal fibrosis. *Artif Cell Nanomed Biotechnol* 2018;**46**:S1016–S1025.
47. Hindi SM, Sato S, Xiong G, Bohnert KR, Gibb AA, Gallot YS, et al. TAK1 regulates skeletal muscle mass and mitochondrial function. *Jci Insight* 2018;**3**: e98441–e98459.
48. Ogura Y, Hindi SM, Sato S, Xiong G, Akira S, Kumar A. TAK1 modulates satellite stem cell homeostasis and skeletal muscle repair. *Nat Commun* 2015;**6**:10123–10139.
49. Cencetti F, Bernacchioni C, Nincheri P, Donati C, Bruni P. Transforming growth factor-beta 1 induces transdifferentiation of myoblasts into myofibroblasts via up-regulation of sphingosine kinase-1/S1P(3) axis. *Mol Biol Cell* 2010;**21**:1111–1124.
50. Xu DQ, Zhao L, Jiang JW, Li SJ, Huang XF, Sun ZR, et al. A potential therapeutic effect of catalpol in Duchenne muscular dystrophy revealed by binding with TAK1. *J Cachexia Sarcopenia Muscle* 2020; https://doi.org/10.1002/jcsm.12581
51. von Haehling S, Morley JE, Coats AJS, Anker SD. Ethical guidelines for publishing in the. *J Cachexia Sarcopenia Muscle* 2019;**10**:1143–1145.